Improved Mechanical Properties of Low Alloyed SinteredSteels through Fe – Mn – Si Master Alloys

A. Marquardt[1],C. Recknagel[1], I. Langer[2], S. Müller[2], B. Kieback[1]

[1] *Institute of Materials Science, Technische Universität Dresden, 01062 Dresden, Germany*
[2] *Schunk Sintermetalltechnik GmbH, Roßtrappenstr. 62, 06502 Thale, Germany*

In recent years cost reduction in powder metallurgy, by using alternative alloying elements, is more and more in focus of interest. Aim of this work is to present that master alloys containing Mn and Si are a practicable alternative to conventional expensive elements like Mo and Ni.
Fe-Mn-Si master alloys were designed with the thermodynamic Software PANDAT, to exhibit a liquid phase at sintering temperature that enables high sintering activity and homogeneous element distribution. Iron powder AHC 100.29 (Höganäs AB) was used and mixed with varying amounts of carbon and 3 m-% of different master alloys. The powders were compacted at 600 MPa and sintered under $90\%N_2/10\%H_2$ at 1140 °C and 1250 °C. Specimens were tensile tested and characterised by light microscopy and SEM+EDX. The results show that, depending on the sintering temperature and powder particle size of the master alloys, improved mechanical properties are obtained by effective alloying, using a transient liquid phase.
Keywords: low alloyed PM-steel, Fe-Mn-Si-Master Alloy, transient liquid phase sintering, mechanical properties

Introduction

Low alloyed sintered steels are still in focus of many researchers. Since a few decades, the aim is to replace the toxic Nickel and the expensive Molybdenum and Copper with cheap elements like Manganese, Silicon and Chromium. Chromium is already established in powder metallurgy processes. Si and Mn (as well as Cr) have a relative high oxygen affinity and Mn itself has as well a low vapour pressure. This is the reason why elementary Manganese first evaporates then oxidises and finally condensates at the particle surface [1, 2, 3]. Due to these facts, Mn and Si are not commonly used in powder metallurgy processes. Hryha et al. [4, 5] analysed the effect of the alloying mode, by using Mn in low alloyed sintered steels. They showed that premixed Mn powder lowered the evaporation of Mn. So it is possible to reach enhanced mechanical properties, in comparison to samples alloyed with electrolytic Mn or ferromanganese. Klein [6, 7] and Zhang [8, 9] studied low melting Fe-Mn-Si Masteralloys (MA). Klein illustrated, that the homogenisation by using MA is quite enough to reach a homogeneous distribution from the alloying elements at the given sintering conditions. Beiss [10, 11] studied also the use of MA. In his work he used an innovative and expensive kerosene atomised Powder, to lower the oxygen amount of the powders. As it is well-known and mentioned above, Mn, Si and Cr have a high oxidation potential. This is the reason why until now, no water-atomised MA-powders were used. Aim of this work is to use low cost water-atomised MA-powders, and to illustrate the beneficial effect of the Master alloying mode.

Experimental procedure

With the support of PANDAT software low melting MA-systems containing Mn, Si, Fe and Cr were calculated. The melting point should be in the range from 1050 to 1200 °C. Table 1 shows the calculated and via DSC experimentally determined liquidus temperatures. There is still a wide gap between calculated and determined temperatures. This gap could be explained, to some extent, by the impurities incorporated in the water-atomising procedure for MA-powders *I*, *II* and *IV*. Such unwanted additions to the Masteralloy could lower the liquidus temperature notably. *MA III* is a gas-atomised powder and thus free of impurities, so the increased liquidus temperature could be explained. Furthermore, the wettability of the used MA were in focus of the authors, therefore experiments (in comparison to Oro [12]) were carried out. For every MA the wetting angle was lower than 25°. So it can be assumed, that there is no sweating out of the specimens.
The water-atomised *MA* (*I,II,IV*) were cast and atomised at a testing plant with a capacity of 50 kg. Afterwards, they were sieved below 45 µm. Whereas *MA III* is, as already mentioned, a gas-atomised powder ($D_{50}=12µm$) thus needs no sieving.

Table 1: Masteralloy analyses, calculated and determined liquidus temperatures

Masteralloy	Fe	Mn	Si	Cr	O$_2$ [m%]	calculated	DSC
I	x	x	x		0,42	1140°C	1110°C
II	x	x	x		0,7	1150°C	1120/1192°C
III	x	x	x		0,06	1150°C	1214°C
IV	x	x	x	x	1,10	1180°C	1147°C

The achieved oxygen contents are shown in Table 1. AHC 100.29 (Höganäs AB, Sweden) was mixed with 3 % MA, 0.3 (*a*) or 0.6 %C (*b*) and 0.8 % lubricant. The resulting chemical compositions are displayed in Table 2. To achieve a comparison between the Masteralloy-technique and binary-alloying-technique compositions *I* and *II* were also mixed with FeMn 80 and FeSi 45 (listed as *FeM*). With a Lauffer HPM 60LS, the specimens were uniaxially pressed at 600 MPa into a tensile testing shape corresponding to DIN EN ISO 2740 and were sintered in a laboratory tube furnace with a heating rate adapted to the industrial process. From RT to 900 °C with 10 K/min, from 900 °C to sintering temperature with 5 K/min (1140 °C or 1250 °C) and sintered for 30 min. The cooling rate was kept constant at 4 K/min; sintering atmosphere was a 90/10 N$_2$/H$_2$ gas mixture with a dew point of approximately -55 °C. Subsequently, all specimens were tensile tested and analysed by light microscopy and SEM and EDX.

Table 2: Chemical composition of investigated specimens

Specimen	C [m%]	Mn [m%]	Si [m%]	Cr [m%]
I a	0,3	1,37	0,57	0
I b	0,6	1,37	0,57	0
II a	0,3	1,37	0,69	0
II b	0,6	1,37	0,69	0
III a	0,3	1,37	0,69	0
III b	0,6	1,37	0,69	0
IV a	0,3	1,37	0,69	0,6
IV b	0,6	1,37	0,69	0,6

Results & Discussion

Chemical Analyses

All specimens were analysed via optical emission spectroscopy (OES) to quantify the change of chemical composition during the sintering stage. For all specimens a carbon loss of approximately 0.1 % was found. Solely for the specimens alloyed with FeMn and FeSi, a loss in Mn (≈ 0.3 %) and Si (≈ 0.2 %) content was detected. It is obvious that the loss in Mn concentration is caused by the low vapour pressure of the Mn during the heating and isothermal holding period [1, 8]. Sintering with FeMn leads to a Mn evaporation, thus the resulting vapour can condensate at the particle surface, or disappear from the specimen in the gaseous state during the sintering stage [1, 2, 3]. The specimens alloyed with the MA have only a loss of 0.08 % Mn and 0.04 % Si. As reported in [8] the sublimation rate of Mn in combination with MA-technique is even lower than for the pure Mn. This is the reason for minimal loss of alloying elements.

Hardness

As it is displayed in Table 3, the hardness of the investigated specimens depends on the alloying mode. Specimens alloyed with the gas-atomised powder (*IIIa* and *IIIb*) attain the highest hardness. The hardness of binary alloyed or water-atomised alloyed specimens is approximately 30-40 HV10 lower. In relation to the uniform cooling rate, and thus the resulting ferritic / perlitic microstructure, and the equal density of the sintered specimens, the homogenisation of alloying elements should be the determining factor. Fig 2 illustrates that there is a huge amount of transient liquid phase (darker areas) which occurs during heating and sintering. As it is well know [6] the interdiffusion-coefficient for alloying elements residing in a liquid phase are much higher than these for elementary alloyed elements.
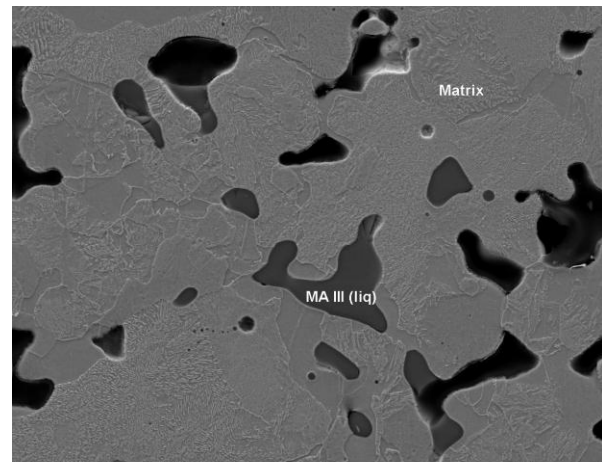
Table 3: HV 10 specimens *II* and *III*, sintered at 1140 °C and 1250 °C, cooling rate 4K/min

	FeM II a		II a		III a		FeM II b		II b		III b	
T_{Sint} [°C]	1140	1250	1140	1250	1140	1250	1140	1250	1140	1250	1140	1250
HV 10	122	121	99	109	122	155	126	127	116	136	158	164
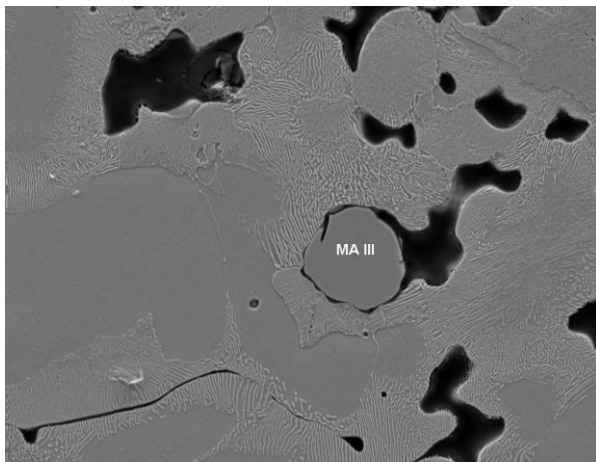
IIIb_1140°C, 15kV, 12mm, 1000x   ⊢— 20 µm —⊣

Fig 1: *IIIa*, remaining *MA III (1140 °C)*

IIIb, 15kV, 13mm, 1000x   ⊢— 20 µm —⊣

Fig 2: *IIIa*, liquefied *MA III (1250 °C)*

It can be estimated, that the homogenisation of Mn and Si for specimen *III* is even higher than for specimen *FeM II*. The high oxygen content of the water-atomised *MA II* could be a reason for the insufficient hardness of the specimens alloyed with 0.3 %C (specimen *a*). It could be possible that an oxide layer at the particle surface of the MA-powders, lowers the diffusion. This hinders the diffusion of the alloying elements from the likewise occurring liquid phase into the iron matrix. The higher carbon content present in specimens *IIb* could be the reason for an increased hardness. At approximately 1000°C the carbon could react with the oxide layers at the particle surface of *MA II*. Thereby the SiO_2 and MnO could be reduced with C, by producing CO/CO_2, Si and Mn. This reaction could "purify" the *MA II* and lower the liquidus temperature of the MA particles, and therewith increase the diffusity of the alloying elements and finally enhance the mechanical properties.
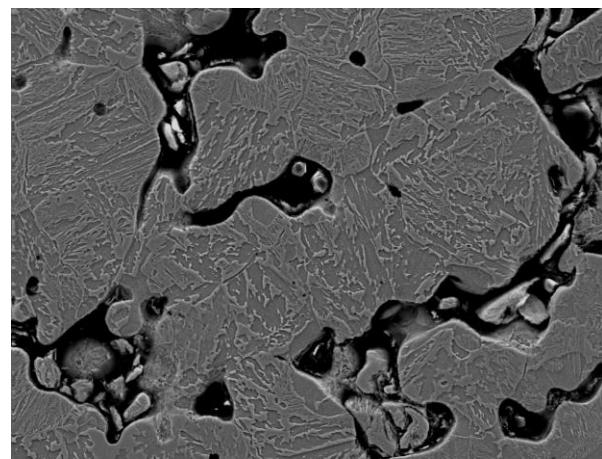
Mechanical properties

The mechanical properties are summarized in Table 4 and 5. It is well-established, that properties depend on sintering conditions, for instance the sintering temperature. At low sintering temperatures, the *FeM* specimens achieve lowest properties. The reason is that, with higher ferromanganese contents the swelling increases during sintering at low temperatures [3, 13]. This indicates the evaporation of Mn and thereby the formation of an iron skeleton. The iron skeleton remains and acts as an impurity. At higher sintering temperatures (1250 °C) the above mentioned iron skeleton disappears completely, pores close, shrinkage sets in and the resulting mechanical properties rise. Fig 3 and 4 indicate this behaviour.
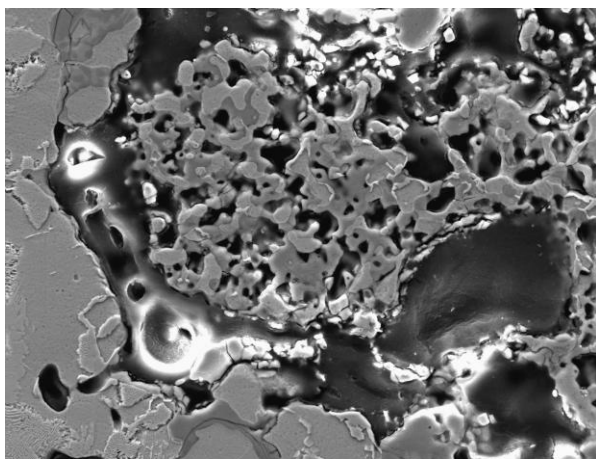
FeM IIa_1140°C, 15kV, 14mm, 1000x   ⊢— 20 µm —⊣

Fig 3: *FeM IIa*, remaining Fe skeleton (1140 °C)

FeM IIa_1250°C, 15kV, 13mm, 1000x   ⊢— 20 µm —⊣

Fig 4: *FeM IIa*, dissolved Fe skeleton (1250 °C)

Table 4: Mechanical properties, elongation, density and shrinkage, sintered at 1140 °C

Specimen	YS [MPa]	TS [MPa]	Elongation [%]	Density [g/cm³]	Shrinkage
FeM I a	140	206	1,44	6,83	-0,63
I a	200	318	3,52	6,93	0,7
FeM I b	--	164	0,18	6,80	-0,22
I b	234	381	2,90	6,89	0,74
FeM II a	--	115	0,08	6,77	-0,92
II a	219	324	3,46	6,86	0,21
III a	191	332	3,13	6,87	0,3
FeM II b	--	125	0,11	6,75	-1,23
II b	227	374	2,77	6,83	0,23
III b	252	339	0,95	6,87	0,47
IV a	183	317	3,41	6,88	0,43
IV b	217	355	1,98	6,84	0,47

Especially for *MA I* there is an interesting behaviour. As can be seen the mechanical properties do not change significantly by changing the sintering temperature. Table 1 provides the evidence; the liquidus temperature determined by the DSC investigations is quite low. The liquid phase forms at 1110 °C so it is possible to use the higher diffusity of alloying elements in the liquid phase at the lower temperatures. Table 4 shows that the shrinkage caused by using the MA is finished at 1140 °C. Fig 5 and 6 corroborate this assessment. The liquid phase formation starts at 1140 °C (Fig 5). The amount of liquid phase in comparison to the other *MA's II, III* and *IV* is quite larger. At 1250 °C only a few areas filled with liquid phase remains are visible. Another benefit is the start of pore rounding, visible at higher sintering temperatures (Fig 6).

Table 5: Mechanical properties, elongation, density and shrinkage, sintered at 1250 °C

Specimen	YS [MPa]	TS [MPa]	Elongation [%]	Density [g/cm³]	Shrinkage
FeM I a	170	266	2,09	6,86	0,25
I a	233	355	3,49	6,92	0,88
FeM I b	235	229	0,38	6,80	0,39
I b	277	393	2,01	6,89	0,89
FeM II a	184	255	1,24	6,81	0,42
II a	220	342	4,3	6,85	0,46
III a	246	366	3,10	6,85	0,11
FeM II b	229	241	0,30	6,78	0,07
II b	278	418	2,51	6,81	0,91
III b	287	419	2,43	6,87	0,74
IV a	211	335	3,90	6,89	0,61
IV b	268	420	2,36	6,85	0,61

The chemical compositions of specimens *II* and *III* (a and b) are equal. The mechanical properties are different in terms of carbon content and atomatisation mode of the MA-powders. Specimens with 0.3 %C (*a*) have only a minor enhancement in properties by increasing the sintering temperature. Gas-atomised powders generate better mechanical properties than water-atomised powders. At 1140 °C the smaller D_{50} of the gas-atomised powder plays an important role. It is obvious that *MA II* creates only a small amount of liquid phase (Fig 7), so the diffusity is not high enough to reach a homogeneous distribution or a complete dissolution of the MA particles.
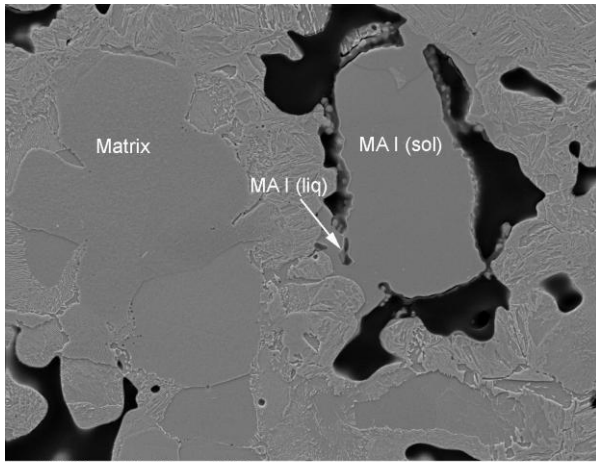
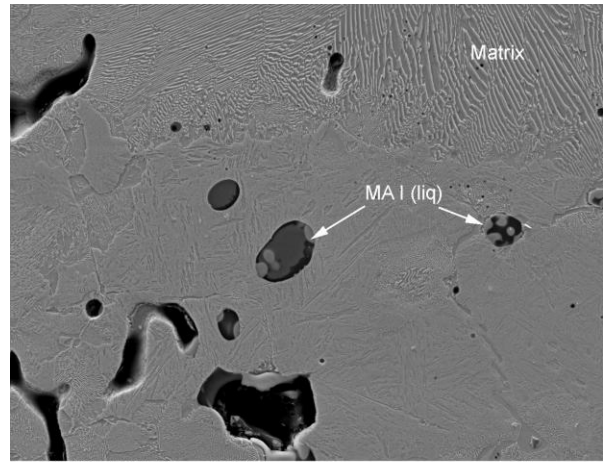Fig 5: *Ia*, formation of liq. phase (1140 °C)

Fig 6: *Ia*, remnants of liq. phase (1250 °C)

In comparison to *MA III* the remnant particles of *MA II* are much larger and so the strength of the specimens is lowered. At higher sintering temperatures *MA II* and also *MA III* particles dissolve completely as shown in Fig 2 and Fig 8. Only a few areas with remnants of liquid phases are visible. Due to the higher oxygen content of *MA II* (Table 1) an enlarged surface oxide layer could decrease the diffusity and homogeneous distribution of the alloying elements. This could be the reason for the minor properties.

The higher Carbon content leads to enhanced properties but also to a decrease in elongation. In comparison to the specimens alloyed with 0.3 %C, a change must be noted: Water-atomised specimens sintered at 1140 °C generate higher mechanical properties. At higher temperatures the gas-atomised powder reaches comparable mechanical properties to the water-atomised powder. As mentioned above, the higher carbon content could reduce the oxides, and thus result in higher mechanical properties at 1140 °C. Fig 7 presents that assumption, small amounts of the liquid phase occurred at the surface of *MA II,* and thus the MA might get connected with the matrix, thereby the pores were also rounded. Remember in Table 1 the liquidus temperature of *MA III* is very high, so it can be assumed that there is no liquid-phase present using *MA III* at 1140 °C. The residual *MA III* in specimens *IIIb* acts, as mentioned above, as impurity. They are not connected with the matrix (Fig 1). At higher sintering temperatures *MA III* also originate a liquid-phase, finally resulting in a homogeneous distribution of the alloying elements (Fig 2). This again provides higher mechanical properties (Table 5).

Specimens produced with the Chromium rich *MA IV* are at the same property levels as the Cr free *MA I*, *II* and *III*. The oxygen enrichment of the *MA IV* (given at Table 1) could be one reason for this effect. With enhanced sintering temperatures (above 1250 °C) or lowering the dew point it could be possible to reduce the Cr-oxide completely to Cr and thereby enhance the mechanical properties. Therefore further investigations are planned.
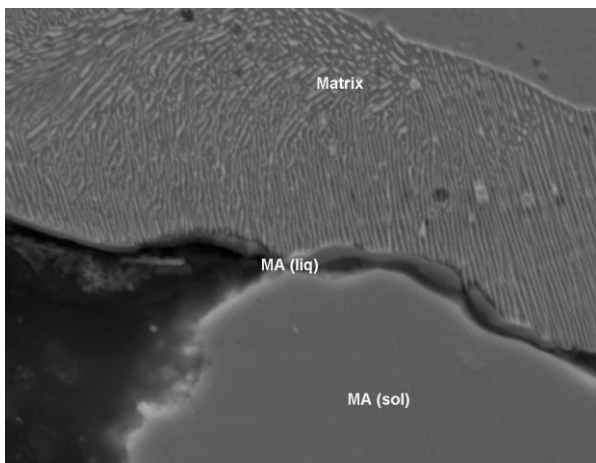

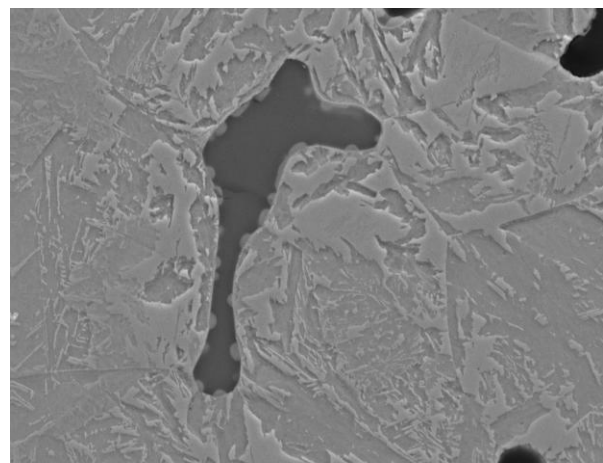Fig 7: Evolution of the liq. phase at the surface (1140 °C)

Fig 8: *IIa,* remnants liquefied *MA II (1250 °C)*

Conclusions

Low alloyed sintered steels alloyed with a transient liquid phase forming MA's are discussed in this paper. It was pointed out that water-atomised MA-powders with acceptable low oxygen contents could be produced. Furthermore, the Mn-evaporation could be eliminated and so the swelling at low temperature sintering cycles also could be lowered. Chemical analysis showed that the steep decrease of Mn and Si by using elemental powders, or binary powders, could be lowered to a minimum by using MA-technique.

There are some influences on the resulting mechanical properties:
- The liquidus temperature of the MA:
    o Low liquidus temperatures result in homogeneous elemental distribution at low sintering temperatures (Specimens *I*)
    o If the MA remains in a solid state, the particle size has a detrimental effect on the properties
- Carbon content:
    o Higher carbon contents result in higher mechanical properties and lower the elongation
    o At higher carbon contents the water-atomised MA could be reduced and thus finally results in higher mechanical properties at lower sintering temperatures

The results show that the utilisation of Fe-Mn-Si leads to enhancement of the mechanical properties. Microstructure developments, heat treatment, and density enhancement are planned.

Acknowledgements

References

[1] A. Šalak, Powder Metall. Int., vol. 18 (1986), no 4; pp: 266-270
[2] A. Šalak, M. Selecká, R. Burec, Powder Metall. Progress, Vol.1 (2001), no 1, pp: 41-57
[3] M. Selecká, A. Šalak, Powder Metall. Progress, Vol.8 (2008), no 1, pp: 7-23
[4] E. Hryha, L. Nyborg, E. Dudrova, S. Bengtsson, World PM 2010, vol 3, pp: 87-94
[5] E. Hryha, E. Dudrova, T. Mizutani, Application of Thermodynamics to biological and materials science, chapter 22: "The sintering behaviour of Fe-Mn-C powder system, correlation between thermodynamics and sintering process, Manganese distribution and microstructure composition, Effect of alloying Mode", pp: 573-603, ISBN: 978-953-307-980-6,
[6] A.N. Klein, R. Oberacker, F. Thümmler, Powder Metall. Int., vol 17 (1985), no 2, pp: 71-74
[7] A.N. Klein, R. Oberacker, F. Thümmler, Powder Metall. Int., vol 17 (1985), no 1, pp: 13-16
[8] Z. Zhang, R. Sandström, Journal of alloys and Compounds 363 (2004), pp: 194-202
[9] Z. Zhang, K. Frisk, A. Salwén, R. Sandström, Powder Metall., vol 47 (2004), no3, pp: 239-245
[10] P. Beiss, Materials properties of Atomet 4401 with 12.5% Melt 11 and 0.5% C, Report no 656, Institute for Materials Science, RWTH Aachen University, 2005
[11] P. Beiss, R. Wassenberg, Proc. Euro PM 2005, PM Low Alloy Steel II, pp: 143-149
[12] R. Oro, M. Campos, A.R. Garcia-Cebadera, J.M Torralba, World PM 2010, vol. 2, pp: 321- 330
[13] H. Danninger, R. Pöttschacher, S. Bradac, A. Šalak, J. Seyrkammer, Powder Metallurgy, vol 48 (2005), no 1, pp: 23-32